New approaches to contrast agent modelling

T G Leighton[1], H A Dumbrell[2]

[1] ISVR, University of Southampton, Southampton S017 1BJ, UK
[2] DSTL, Winfrith Technology Centre, Dorchester, Dorset, DT2 8WX, UK

Abstract. Current options for modelling contrast agent nonlinearities do not predict acoustic propagation. Other popular formulae are restricted to the linear steady state (*e.g.* for cross-sections, sound speed and attenuation). Hence all options for modelling contrast agents have limited applicability to most of the insonification conditions to which they are exposed *in vivo*. This paper provides a theoretical framework into which any nonlinear single-bubble model can be input, to predict the sound speeds and attenuations which clouds of contrast agents would produce. These two propagation characteristics are fundamental to the quantitative interpretations of signals from contrast agents in the clinical environment.

1. Introduction: Two routes to modelling of contrast agent acoustics

There are currently two main classes of theoretical descriptions for ultrasonic contrast agents. The first class involves empirical acoustic scatter cross sections. A cross-section is associated with each harmonic (at frequency ω, 2ω, 3ω etc.). These are based on the ratio of the measured power scattered at the frequency in question, to the intensity of the incident wave (assumed to have a frequency ω). The advantage of this approach is that it is simple, easily related to measurement, and deals with the populations in which contrast agents usually occur. The disadvantages are however considerable. The approach provides a very limited, if any, description of propagation (there would for example be no way of inferring the sound speed from them). As with all cross-sections, the parameter becomes undefined when the driving amplitude is zero, making it unsuitable for many of the short-pulse exposures to which contrast agents are subjected *in vivo*. There is no way to relate this empirical description to the single-bubble dynamics (so that for example the observer does not know how much of a measured 2ω signal arises from bubbles resonant at the driving frequency ω and whose wall pulsations contain a component at 2ω, and how much comes from smaller bubbles whose fundamental pulsation resonance is at 2ω). This weakness arises because the empirical approach is not grounded in the fundamental physics, a factor which leads to its most serious failing. The potency of acoustic cross sections lies in their additive nature, in that the effect from a bubble population can be obtained through a summation of the cross sections of the individual bubbles present (which is similarly the basis of inversions to determine the bubble population from the measured acoustic characteristics). This property comes from the fact that the scattered (or absorbed) powers are additive, which in turn relies on the fact that the signals from the various bubbles in the population are incoherent at the receiver. However by ascribing a cross-section to each harmonic, this basic principle is violated, in that the 2ω signal from any individual bubble will be correlated with the ω signal from the same bubble at the receiver. Hence great caution must be exercised over how the empirical cross sections are utilised.

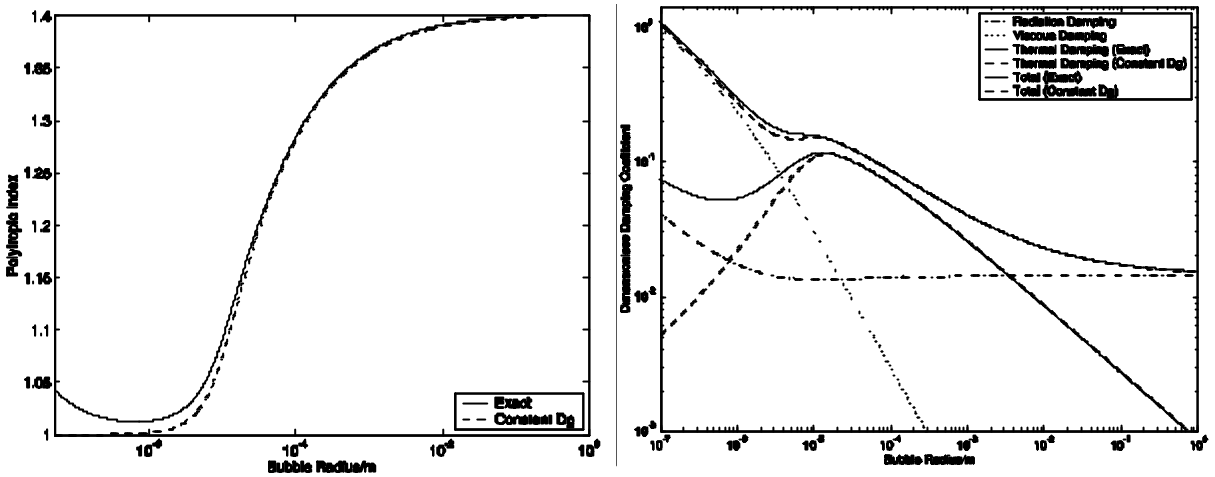

(a) *(b)*

Figure 1. (*a*) The variation of polytropic index with equilibrium bubble size for free air bubbles in water under room conditions, for bubbles driven in the linear syteady state limit at resonance. The dashed line shows the prediction if a constant value is taken for the thermal diffusivity D_g, and the solid line shows the predictions when the effect of Laplace pressure on D_g is included. (*b*) The dimensionless damping constants for bubbles pulsating in the same limit as in (*a*), plotted for an assumed constant D_g (dashed line; plotted thick for thermal damping constant, and thin for total damping constant). This can be compared with the results when the effect of Lapace pressure on D_g is included (solid line; plotted thick for thermal damping constant, and thin for total damping constant). Since these plots relate to linear steady-state pulsations fo bubbles in response to monochromatic forcing, they will in many circumstances be inapplicable for contrast agent exposure. Figure by TG Leighton and PR White.

The second approach to modelling the acoustic properties of contrast agents is through the adaptation of existing models for the dynamics of single bubbles to incorporate wall effects relevant to contrast agents. Whilst on occasion a linear model is used, most often a nonlinear model is adapted. There are two main issues here. First, the limitations of the eventual model will be derived in part by those of the progenitor model. A Rayleigh-Plesset basis will therefore usually provide only for viscous damping, with formulations from the Herring-Keller/Keller-Miksis or Gilmore-Akulichev families being required to incorporate radiation damping. Thermal damping is of particular interest, in that none of the above formulations in themselves include any net thermal losses. Attempts to do this by adding a "thermal viscosity" included no new physics beyond that found in the monochromatic steady-state damping constants, which are of course inappropriate for the exposure of contrast agents to pulses of microseconds-order duration and O(MPa) amplitudes. Thermal damping for the time-dependent nonlinear oscillations of bubbles requires more rigorous treatments [1,2]. A common route is to neglect those damping mechanisms which have proved to be more difficult to incorporate, but this can of course only be done when a quantitative and accurate argument has been made to show that such neglect does not affect the interpretation of the results.

Of particular interest in this context is the common use made of the polytropic index (the ratio of the specific heat of the gas at constant pressure to that at constant volume). This is not a fundamental quantity, but by allowing it to take a value intermediate between the adiabatic case and unity (corresponding to isothermal bubble pulsations), it may be used to adjust stiffness of gas to account for heat flow across the bubble wall. However unless its value varies during the oscillatory cycle, there are no net thermal losses and the polytropic index does not describe net thermal losses. Its characteristics have particular significance for contrast agents, the two reasons. First, the major effort in adapting single-bubble models to contrast agent use has been in order to adapt the stiffness term (which otherwise is dominated by the polytropic characteristics of the gas) to account for the presence of the

agent's wall. Second, the received wisdom about the polytropic index, which has served the macroscopic bubbles community well for decades, does not hold for microscopic bubbles. For example, a widely-held view is that for free air bubbles in water at resonance, the polytropic index tends to the adiabatic limit for large (*i.e.* mm-sized) bubbles, but to the isothermal limit for small (*i.e.* micron-sized) bubbles. This is because the assumption is almost always made that the thermal diffusivity of the gas can be set at a constant value. However the Laplace pressure for micron-sized free bubbles becomes so great as to change the thermal diffusivity of the gas [3], and inclusion of this effect changes the polytropic index and the thermal damping (Figure 1). The wall properties of contrast agents can vary from cases resembling the free-bubble conditions of Figure 1, to ones where an assumption of convenience is made, in which the wall engenders within the bubble a pressure identical to that found far from the bubble (effectively counterbalancing surface tension). The range of assumptions that may be made about gas behaviour in microbubbles needs critical examination.

Whilst these two descriptive routes (empirical cross sections and single-bubble models) are very different, they share a same basic limitation. Specifically, neither can describe key propagation characteristics, such as sound speed and attenuation. These are fundamental to any quantitative interpretation of the acoustic signals from contrast agents. Without a sufficiently accurate knowledge of the sound speed, the range inferred from travel times is misleading. Without knowledge of the acoustic attenuation, quantitative interpretations based on signal amplitude are compromised. Hence the unexpected conclusion, given the title of this section, is that neither class of model will actually describe the acoustics of contrast agents, merely their wall dynamics and radiated pressure fields. In order to obtain information about the propagation of acoustic waves through a contrast agent suspension, another model must be found. Since, as the next section will outline, no such model currently exists, such provision is the purpose of this paper.

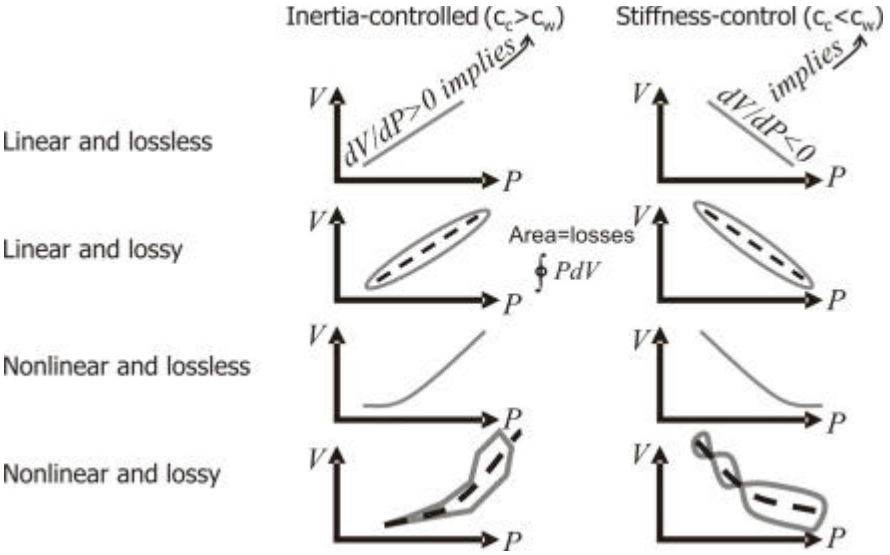

Figure 2. Schematics of steady-state bubble volume oscillations vs. applied pressure. The left column shows the result for the inertia-controlled regime, and the right column corresponds to the stiffness controlled regime. The four rows correspond to conditions which are (from top downwards): linear and lossless; linear and lossy; nonlinear and lossless; nonlinear and lossy.

2. Models for propagation through contrast agent populations

In 1989 Commander and Prosperetti [4] produced the most widely-used formulation for predicting the propagation characteristics of an acoustic wave through bubbly liquids. Its applicability for contrast agents *in vivo* is limited, since the theory assumes linear steady-state bubble pulsations in response to a monochromatic driving field. Leighton *et al.* [5,6] developed a theoretical framework into which any single-bubble model could be input, to provide propagation characteristics (*e.g.* attenuation and sound speed) for a polydisperse bubble cloud (which may be inhomogeneous) incorporating whatever features (*e.g.* bubble-bubble interactions) are included in the bubble dynamics model. Because of the inherent nonlinearity, such a model cannot make use of many familiar mathematical tools of linear acoustics, such as Green's functions, complex representation of waves, superposition, addition of solutions, Fourier transforms, small-amplitude expansions etc. The crux of

this model is in the summation of the volume responses of the individual bubbles to the driving pressures. If the contrast agent cloud is divided into volume elements, let dP_l is the change in the pressure applied to the l^{th} volume element as a result on an incident ultrasonic field. Divide the polydisperse bubble population into radius bins, such that every individual bubble in the j^{th} bin is replaced by another bubble which oscillates with radius $R_j(t)$ and volume $V_j(t)$ (about equilibrium values of R_{0_j} and V_{0_j}), such that the total number of bubbles N_j and total volume of gas $N_j V_j(t)$ in the bin remain unchanged by the replacement. If the bin width increment is sufficiently small, the time history of every bubble in that bin should closely resemble $V_j(t) = V(R_{0_j}, t)$ (the sensitivity being greatest around resonance). Hence the total volume of gas in the l^{th} volume element of bubbly water is $V_{g_l}(t) = \sum_{j=1}^{J} N_j\left(R_{0_j}, t\right) V_j(t) = V_{c_l} \sum_{j=1}^{J} n_j\left(R_{0_j}, t\right) V_j(t)$, where $n_j\left(R_{0_l}, t\right)$ is the number of bubbles per unit volume of bubbly water within the j^{th} bin. From this scheme Leighton *et al.* [6] identified a parameter: $x_{c_l} \approx c_w \Big/ \sqrt{1 - r_w c_w^2 \sum_{j=1}^{J} n_j\left(R_{0_j}\right)\left(dV_j / dP_l\right)}$. Crucially this x_{c_l} provides a *generic framework into which any bubbly dynamics model may be inserted* (giving $dV_j(t)/dP_l(t)$ appropriate to bubbles in free field or reverberation, *in vivo*, in structures or sediments, or in clouds of interacting bubbles, etc. as the chosen model dictates). To illustrate this, consider a monodisperse bubble population pulsating in the linear steady-state (Figure 2). If the propagation were linear and lossless, the graphs of applied pressure (*P*) against bubble volume (*V*) would take the form of straight lines, the location of the bubble wall being plotted by the translation of the point of interest up and down these lines at the driving frequency (Figure 2, top row). Since a positive applied pressure compresses a bubble in the stiffness regime, here $dV/dP<0$ (Figure 2, top row, right). If, in this linear lossless regime, x_{c_l} (above) is seen as equivalent to c_c (the sound speed in the bubbly water), then $c_c < c_w$. However since a p phase change occurs across the resonance, the opposite is true in the inertia-controlled regime (Figure 2, top row, left). The sound speed in a polydisperse population can be found through addition of such gradients as directed by the formula for x_{c_l} (above). If conditions are linear and lossy (Figure 2, second row), each acoustic cycle in the steady-state must map out a finite area which is equal to the energy loss per cycle from the First Law of Thermodynamics [6]. The characteristic spine (dashed line, Figure 2, second row) of each loop can, through summation as directed by the formula for x_{c_l}, give the sound speed in a polydisperse population. This is effectively equivalent to the approach of Commander and Prosperetti [4], although they characterised the problem using a complex wavenumber, rather than through the locus in *P-V* space. It is interesting to note that Commander and Prosperetti found greatest difficulties with their theory when strong bubble resonances occur: The middle row of Figure 2 illustrates how this will coincide to conditions where not only is the area mapped out very large, but the characteristic gradient of *dV/dP* is very difficult to identify (in keeping with known through-resonance behaviour of sound speed in monodisperse populations). If conditions are nonlinear and lossless, in steady-state the *P-V* graphs will depart from straight-lines (for example because the degree of compression cannot scale indefinitely; Figure 2, third row). The gradient *dV/dP* varies throughout the acoustic cycle in a manner familiar from nonlinear acoustic propagation, and appropriate summation (as in x_{c_l}) can appropriately describe this propagation and the associated waveform distortion. If conditions are nonlinear and lossy, finite areas are mapped out, and whilst the characteristic spines may present significant challenges, nonlinear propagation may again be identified (the example of the right of the bottom row in Figure 2 illustrates

a strong third harmonic, where the steady-state volume pulsation undertakes three cycles for each period of the driving field).

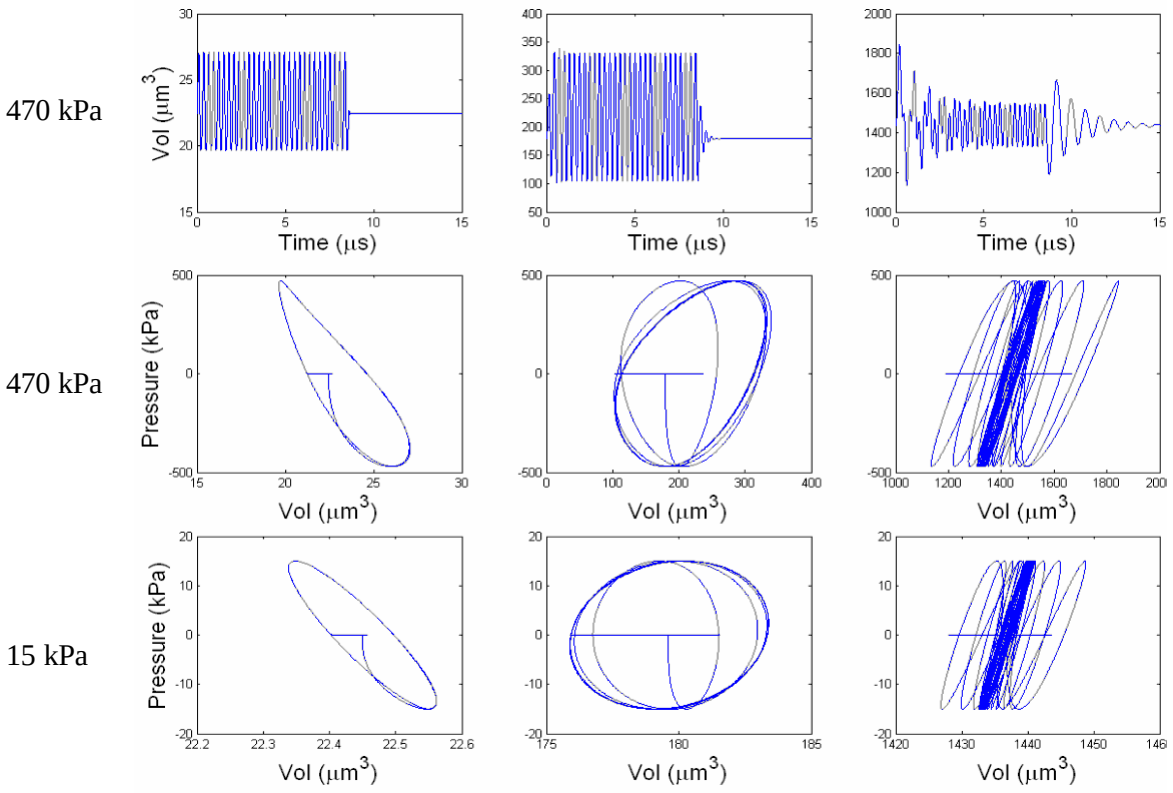

Figure 3 Volume time histories (top row) and *P-V* plots for Optison, as modelled by the Rayleigh Plesset equations with wall conditions as described in text. The bubble is insonified by a 3.5 MHz pulse of 30 cycles duration and 0-peak amplitude of 470 kPa (top and middle rows) and 15 kPa (bottom row).

3. Results

Whilst Figure 2 showed a schematic of the steady-state solutions, Figure 3 plots (top row) the volume time history, and (middle) the time-dependent *P-V* graphs, for the 3.5 MHz insonification of initially motionless bubbles (either side of the 3.5 *mm* resonance) by a pulse of 30 cycles duration, and 0-peak amplitude 0.47 MPa. This amplitude is chosen to coincide with the conditions of Coussis *et al.* [7], who used linear steady-state theory. The differences from such theory for this model is illustrated by comparison of the middle row with the bottom, where the 15 kPa driving amplitude will (in the steady state) give a result close to the linear model. Note how, during ring-up, the characteristic spine may differ from that associated with the steady-state solution (e.g. (*b*) in middle row). After the cessation of the driving pulse the *P-V* plot maps out a straight line as the bubble volume rings down. Whilst Leighton *et al.* [6] modelled free bubbles with full nonlinear damping, the calculations in this paper are based on inclusion of appropriate wall parameters (after Church [8]) in the Rayleigh-Plesset model, and includes viscous and thermal damping (after [1,2]). Future models will also incorporate radiation damping. At higher driving amplitudes (Figure 4, top and middle rows) the results deviate further from the 15 kPa limit (Figure 4, bottom row).

4. Conclusions

The model of this paper represents a significant advance on previously-available models for contrast agent acoustics (Table 1). It will allow the first assessment of the propagation of novel pulsing regimes for contrast agents and, for example, the propagation of lithotripter pulses through cavitation clouds.

Acknowledgements
The authors wish to acknowledge support from DSTL and EPSRC (GRN19243/01).

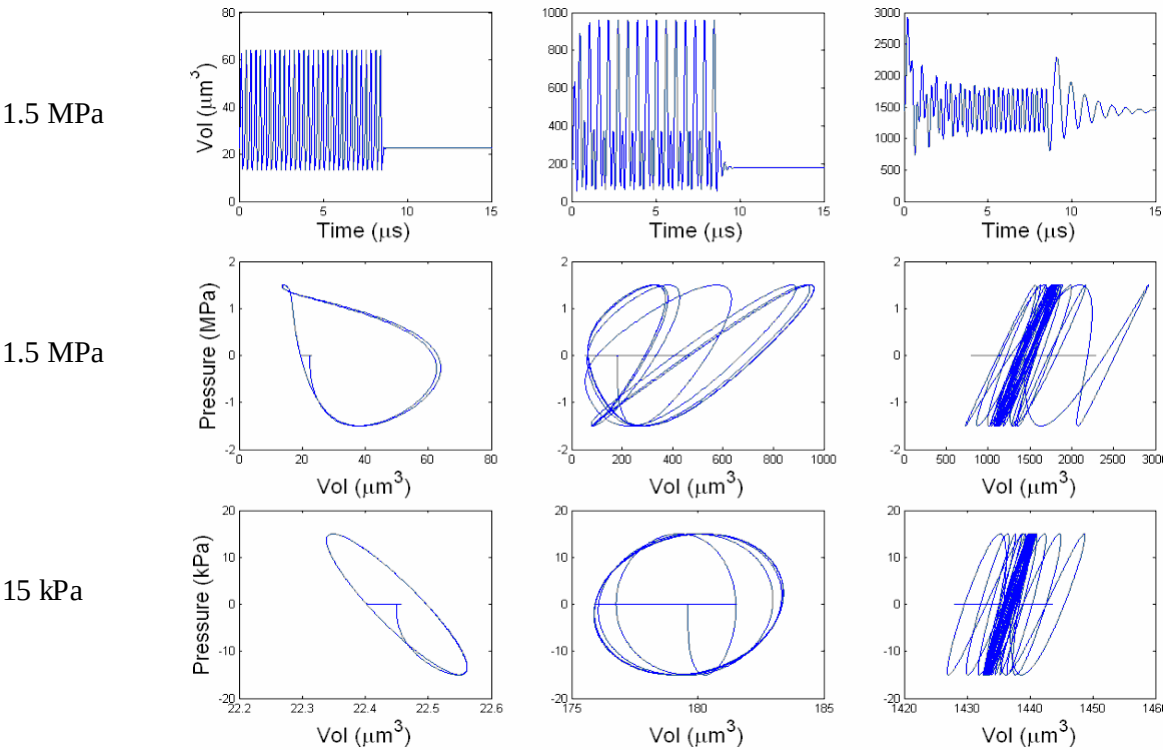

(a) 1.75 mm *(b) 3.5 mm* *(c) 7.0 mm*

Figure 4. As for Figure 3, but with top and middle rows driven with a 1.5 MPa (0-peak) field.

Model type	Arbitrary Driving pulse	Transient period	Non-linear damping	Harmonics/ Subharmonics	Scattered pressures	Atten-uation	Population effects	Tissue effects
(i)	No	No	No	←←←←←←Empirical? ? ? ? ?			Empirical	No
(ii)	Monochromatic	No	←←←←←←Only in linear steady state ? ? ? ? ?				No	No
(iii)	Yes	Yes	See †	Yes	Yes	No	No	No
(iv)	Yes	Yes	Yes	Yes	Yes	Yes	Yes	Yes

Table 1. Summary of properties of the models discussed in this paper, for (i) Empirical Cross-section, (ii) Linear steady-state propagation model, (iii) Nonlinear single bubble plus wall effects, (iv) Leighton *et al.* [6]. (Note †: Potentially yes, but often only for viscous damping).

5. References

[1] Nigmatulin R I, Khabeev N S, and Nagiev F B 1981 *Int. J. Heat Mass Transfer*, **24**, 1033
[2] Prosperetti A and Hao Y 1999 *Phil. Trans. R. Soc. Lond. A* **357**, 203
[3] Leighton T G 1994 *The Acoustic Bubble* (Academic Press) §3.4.2b(iv)
[4] Commander K W and Prosperetti A 1989 *J. Acoust. Soc. Am.* **85**, 732
[5] Leighton T G 2001 *J. Acoust. Soc. Am.*, **110**, 2694
[6] Leighton T G, Meers S D and White P R 2004 *Proceedings of the Royal Society A* (in press)
[7] Coussis C-C, Holland C K, Jakubowska L, Huang S-L, MacDonald R C, Nagaraj A and McPherson D D 2004 *Ultrasound in Medicine and Biology*, **30**, 181
[8] Church C C 1995 *J. Acoust. Soc. Am.* **97 (3)**, 1510